Research Square

Preprints are preliminary reports that have not undergone peer review.
They should not be considered conclusive, used to inform clinical practice,
or referenced by the media as validated information.

Response modification factor of SMA-based self-centering buckling-restrained braced frames

Nader Hoveidae

hoveidaei@azaruniv.ac.ir

Azarbaijan Shahid Madani University https://orcid.org/0000-0001-6449-1177

Samaneh Abbasi

Azarbaijan Shahid Madani University

Research Article

Keywords: Steel braced frame, Buckling-restrained brace, Shape memory alloy, self-centering, Response modification factor, fragility

Posted Date: August 24th, 2023

DOI: https://doi.org/10.21203/rs.3.rs-3217308/v1

License: This work is licensed under a Creative Commons Attribution 4.0 International License.
Read Full License

Response modification factor of SMA-based self-centering buckling-restrained braced frames

Nader Hoveidae[1*], Samaneh Abbasi[2]

1*- Associate Professor, Civil Engineering Department, Azarbaijan Shahid Madani University, Tabriz, Iran,
Email: Hoveidaei@azaruniv.ac.ir
2- Graduate Student, Civil Engineering Department, Azarbaijan Shahid Madani University, Tabriz, Iran
Email: gh.sama.abbasi@gmail.com

Abstract

Shape Memory Alloys (SMAs) have significant efficacy in seismic resilience design due to their excellent superelasticity. The key characteristics of Nickle-Titanium (Ni-Ti) SMA include desirable fatigue and corrosion resistance and outstanding self-centering capacity, which provides the ability to undergo large deformations while reverting back to their original undeformed shape. The current numerical study presents an innovative Buckling-Restrained Brace (BRB) including a reduced-length core (HSCBRB) that is attached to a robust steel pipe. The core is laterally supported and consists of a SMA rod inserted into a steel pipe. The paper represents a detailed description of the proposed device. The research is carried out by investigating the overall behavior of the structural system as well as taking a close look at the response parameters of the system. In order to evaluate the response modification factor of the steel braced frames, static pushover, nonlinear time history, and incremental dynamic analyses are performed in the OpenSEES environment. Additionally, the fragility response curves are developed and compared. As a result, the proposed device significantly reduces the residual drift response of the steel buckling-restrained braced frames. Furthermore, an average response modification factor of 8.5 is obtained for the SMA-based self-centering buckling-restrained braced frames.

Keywords: Steel braced frame; Buckling-restrained brace; Shape memory alloy; self-centering, Response modification factor, fragility

1. Introduction

BRBs are widely used in high seismicity zones and deliver outstanding ductility and excellent energy-dissipating capacity. The idea of BRB was first proposed in the 1970s when research successes were reported in Japan and India. Several investigations on the seismic response of BRBs can be found in the literature. The first physical sample of a BRB was fabricated and tested by Watanabe et al. (1988). Black et al. (2002) investigated the response of BRBs and

it was concluded that the BRBs possess symmetric and stable hysteretic behavior. The high ductility capacity of the BRBs was reported by Kim and Choi (2010). Walter et al. (2010) designed and analyzed the buckling-restrained braced frames (BRBFs) equipped with SMA and energy-absorbing components. Due to the superelasticity of SMA material, the system exhibited a self-centering response and high energy dissipation capacity. Fahnestock et al. (2003) evaluated the seismic response and maximum ductility capacity of the BRBFs. Prinz and Richards (2012) investigated and compared the seismic performance of BRBFs with eccentric configuration (BRBF-Es) and conventional Eccentrically Braced Frame (EBFs) and it was concluded that the residual drifts in the BRBF-Es were generally greater than those in EBFs. The potential of using an aluminum alloy core in BRBs was experimentally investigated by Avci-Karatas et al. (2018). Asgarian and Moradi (2011) examined the seismic response of the BRBFs incorporating steel and shape memory alloy braces. Results designated the outstanding ability of SMA braces to significantly reduce the residual drifts. An investigation of the seismic behavior of a self-centering bracing system including an SMA bar was conducted by Ghowsi and Sahoo (2020). The SMA rods combined with a steel core significantly increased the self-centering capacity of the brace and reduced the permanent drift response of the BRBFs. Atlayan and Charney (2014) introduced a hybrid BRB that could successfully decrease the residual drift response of BRBFs. An SMA-based novel device for dissipating seismic energy with a significant self-centering capacity was introduced by Eatherton et al. (2014). Moradi et al. (2014) examined the behavior of four-story braced frames. The study reveals a satisfactory performance at the design intensity level. Furthermore, the results indicated that the SMA braces lead to a uniform distribution of inelastic response over the height of the buildings, as well as mitigating seismic response in terms of maximum inter-story drift and residual roof displacement. Furthermore, Hoveidae et al. (2015) introduced a reduced-length BRB that could successfully decrease the permanent drift response of the BRBFs. The seismic behavior of BRBFs equipped with short-length BRBs was investigated by Pandikkadavath and Sahoo (2016) and the proposed device significantly reduced the residual drifts of the braced frames. Bertro introduced the method of incremental nonlinear dynamic analysis (IDA) in 1977 (Popov and Pister 1980). Since the introduction, IDA method was utilized for various applications by many researchers (Nassar and Krawinkler 1991, Bazzaz et al. 2015, Bazzurro and Cornell 1994, Luco and Cornell 1998, Mehanny and Deierlein 1999, Luco and Cornell 2000, Yun et al. 2002, Hakim et al. 2011, Mohammadhassani et al. 2012). Response modification factor of steel frames utilizing SMAs was investigated by Ghassemieh and Kargarmoakhar (2013). The studies designated that seismic response of Chevron bracing is preferable when compared with diagonal X bracing resulted from IDA analysis. Seismic behavior of BRBF structures

is studied and compared with special concentric braced frames (SCBF) by Khorami et al. (2017). Results obtained by performing incremental dynamic analysis (IDA), indicated that structures with high altitude with the possibility of exceeding the collapse prevention performance level, further than lower altitude structures.

The cyclic behavior of BRBs equipped with SMA bars was investigated by Wang and Zhu (2018) and the significant self-centering potential of the proposed brace was reported. Hashemi et al. (2021) explored the seismic behavior of SMA-based self-centering BRBFs and reported a significant reduction in the permanent drift response of the prototype frames. Hoveidae (2019) proposed a novel multi-core BRB with different material arrangements of the core. Compared with the conventional BRBs, the proposed device significantly reduced the residual drift response of the BRBFs subjected to Design-Basis Earthquakes (DBEs) and Maximum Considered Earthquakes (MCEs). Several numerical investigations were conducted to evaluate the self-centering potential of SMA-based hybrid BRBs and consequently, smaller residual drift demands compared with conventional BRBs were reported (Nazarimofrad and Shokrgozar 2019; Dong et al. 2019; Qiu et al. 2020). In another study, the seismic response of SMA-based self-centering buckling-restrained braced frames with optimized length and area of the SMA bars was investigated (Ghowsi and Sahoo 2020). Furthermore, Ghowsi et al. (2020) investigated the seismic response of BRBs including iron-based shape memory alloy cores. The iron-based BRB showed a promising hysteretic response with high fatigue fracture life. Hoveidae and Radpour (2021) numerically investigated the seismic performance of a novel hybrid BRB. The application of a multi-material short-length core resulted in high post-elastic stiffness of the brace. As a result, the proposed device could successfully decrease the residual drift demands in BRBFs. The seismic performance of a double-yield BRB was investigated by Hu et al. (2022) and the high energy dissipation capacity of the brace was reported.

Recently, the mitigation of post-earthquake residual displacement of buckling-restrained braced frames has concerned wide attention. Various solutions have been offered at either the component level or the system level. At the component level, the application of short-core BRBs (Hoveidae et al. 2015; Pandikkadavath and Sahoo 2016), hybrid BRBs (Atlayan and Charney 2014; Hoveidae and Radpour 2021), and SMA-based self-centering BRBs (Asgarian and Moradi 2011; Eatherton et al. 2014; Nazarimofrad and Shokrgozar 2019; Dong et al. 2019; Qiu et al. 2020; Ghowsi and Sahoo 2020; Miller et al. 2012; DesRoches et al. 2004; Wang et al. 2017) have been proposed. At the system level, typical examples include the application of dual buckling-restrained braced frames (Kiggins and Uang 2006), high-strength steel frames (Ke and Chen 2016), and self-centering frames (Qiu and Zhu 2020; Tian and Qiu 2018).

The superelasticity property of SMAs plays an essential role in designing seismic resilient structures. Superelastic SMA bars exhibit a promising self-centering response characterized by a flag-shaped hysteretic curve. In addition to the self-centering potential, SMA bars possess high corrosion resistance and significant fatigue endurance that make them desirable for seismic applications.

The potential of using SMA components to reduce residual drifts has been supported by experimental works (Eatherton et al. 2014; Hoveidae et al. 2015; Pandikkadavath and Sahoo 2016; Wang and Zhu 2018) and numerical studies (Asgarian and Moradi 2011; Ghowsi and Sahoo 2020; Atlayan and Charney 2014; Eatherton et al. 2014; Hoveidae et al. 2015; Pandikkadavath and Sahoo 2016; Wang and Zhu 2018; Hashemi et al. 2021). Efforts can be classified at either the component level or the system level. At the component level, several SMA-based self-centering devices were proposed (Eatherton et al. 2014; Miller et al. 2012; Qiu and Du 2020). At the system level, Fang et al. (2018) used SMA ring springs at the moment-resisting frames and Asgarian and Moradi (2011) used SMA braces to reduce residual drifts of BRBFs. Furthermore, Shams and Ghobadi (2021) investigated the seismic response of a combined SMA-braced frame with BRBF. The studies designated that the permanent drifts could be well reduced.

In addition to the promising self-centering capacity of the former SMA-based BRBs, the proposed devices typically included a self-centering mechanism consisting of pre-stressed wires or rods attached to the buckling-restraining mechanism with significant complexity in detailing and assembly (Eatherton et al. 2014; Ghowsi and Sahoo 2020; Miller et al. 2012). Hence, more efforts can be directed toward the development of SMA-based self-centering BRBs with fewer manufacturing and assembly complexities. Asgarian et al. (2021) studied response modification factor of steel braced frames equipped with smart hybrid re-centering device through conducting IDA. Results implied that proposed hybrid system increases response modification factor compared to SMA simple device while the recentering capability is assured and design problems are reduced to minimum. Ke et al. (2022) develops a performance-spectra-based method to evaluate the seismic performance of industrial steel moment resisting frames (MRFs) with shape memory alloys (SMAs) considering multiperformance indicators and hysteresis transition. By comparing essential structural seismic response quantities predicted by the proposed method with those calculated by nonlinear-response-history analyses (NL-RHAs), the effectiveness of the proposition was confirmed. Seismic performance of steel BRBFs including SMA materials was evaluated by Kazemi and Jonkowski (2023). Results indicated that viscous dampers and SMAs can decrease the values of maximum moment and rotation of hinges of structural members. Furthermore, seismic collapse assessment of hybrid self-centering piston-based braced Frames (SC-PBBFs) equipped with SMA

bars and friction springs was investigated by Rahgozar and Alam (2023). The R-factor value of 8 was recommended for the design of SC-PBBFs at maximum considered earthquake (MCE) level event since the designed archetypes could satisfy the acceptance criteria. Seismic optimization design of BRBFs for uniform damage criterion was proposed by Wu et al. (2023). Results indicated that the damage degree distribution could be effectively controlled by optimizing the BRBs' initial stiffness distribution using an intelligent algorithm.

This paper introduces a novel SMA-based short-length BRB in which the BRB core consists of an SMA rod inserted into a steel Circular Hollow Section (CHS) member. The short-length core is laterally supported by a restraining mechanism and is serially attached to a robust elastic member. Therefore, the brace member is a kind of hybrid device. In the proposed Hybrid Short-Core BRB (HSCBRB), the short-length steel core is expected to deliver a wide hysteretic force-deformation response with a significant strain-hardening capacity. In contrast, the short-length SMA core exhibits a flag-shaped hysteretic behavior. The hysteretic behavior of the proposed brace is expected to be characterized by a combined hysteretic response of the steel and SMA cores. Therefore, the steel core can provide a desirable energy dissipation capacity, whereas the SMA core results in a self-centering response of the brace. The reduced residual deformation of the proposed brace originates from the outstanding self-centering property of the SMA core together with the high post-elastic stiffness of the short-length steel core. In addition, due to the high cost of SMAs, the use of a shorter SMA core, compared with the long one that was typically employed in the previously proposed self-centering BRBs (Eatherton et al. 2014; Ghowsi and Sahoo 2020; Miller et al. 2012) seems economically more affordable.

This paper first characterizes the components and the summarized design methodology of the HSCBRB. Subsequently, the seismic response of the proposed buckling-restrained braced frames is evaluated by nonlinear time history analysis. Afterward, by performing the incremental dynamic analysis (IDA), the response modification factor of the proposed BRBF system is evaluated.

2. HSCBRB concept and detailing

The concept of hybrid BRBs to reduce the residual drifts of BRBFs has been investigated by several research studies (Atlayan and Charney 2014; Hoveidae 2019; Hoveidae and Radpour 2021). In this paper, the conceptual SMA-based BRB, which consists of a reduced-length double-core BRB that is attached to an elastic member, is expected to provide significant post-elastic stiffness and outstanding self-centering capacity. Fig. 1 characterizes the detailed components

of the proposed HSCBRB. The core member is composed of a steel Circular Hollow Section (CHS) member and an SMA rod parallelly inserted into the steel core. For the fabrication of the hybrid core, first the inner surface of the steel core is threaded together with the outer surface of the SMA rod. Consequently, the SMA rod and the steel core are attached together through the threaded surfaces. The composite core is supposed to be connected to the end and middle plates through a weld joint at the end of the steel core. The buckling-restraining mechanism of the hybrid core includes the inner and the outer sleeves made by steel CHS members together with the restrainer disks, as shown in Fig. 1. To prevent the undesirable local buckling response of the hybrid core at the end of the brace, a steel collar is used. The circumferential restrainer disks organized and equally spaced (welded) at the outer surface of the inner sleeve are employed to transfer the normal contact forces that are developed between the core and the encasing. A rigid connection by a groove weld is assumed between the elastic part and the middle plates, as shown in Fig. 1. As depicted in Fig. 1, the bolted middle connection of the brace allows for simple replacement of the damaged short-length core after severe earthquakes.

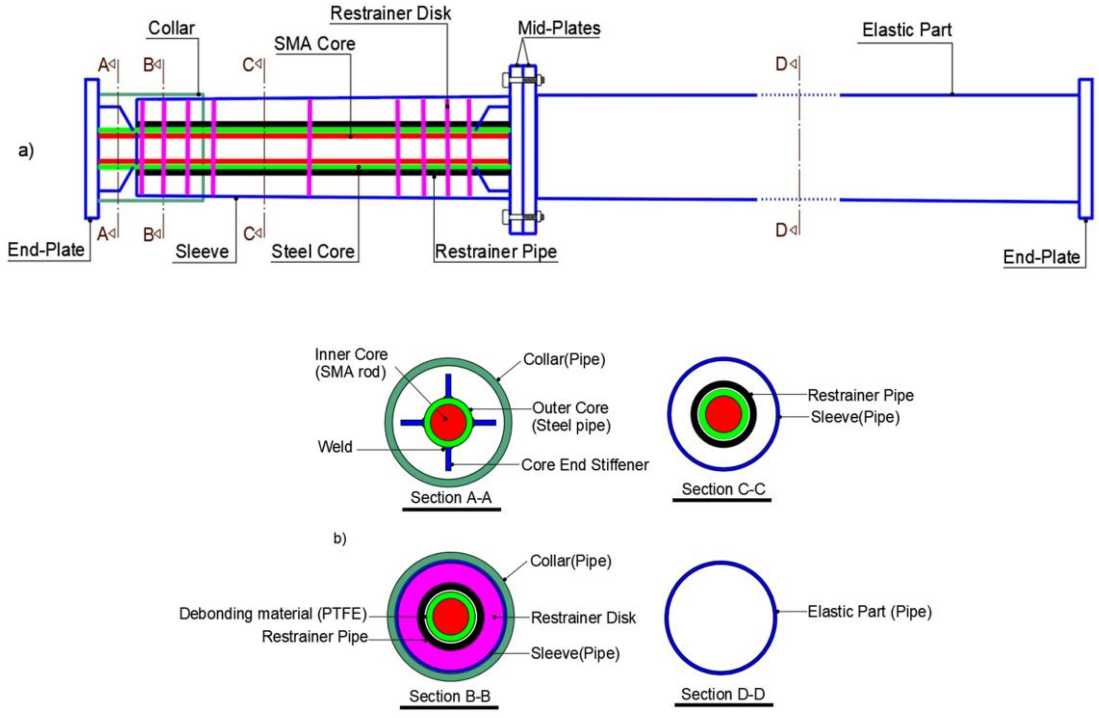


Fig. 1. Components of the proposed HSCBRB; a) longitudinal view; b) cross-sectional view

3. Critical core length of HSCBRB

As discussed in the preceding section, the proposed HSCBRB includes a composite short-length core attached to an elastic member. In comparison to conventional BRBs, a higher axial strain demand is expected for a BRB including a shorter core. Though the SMA material shows excellent low-cycle fatigue life (Vafaei and Eskandari 2016), the steel material is prone to low-cycle fatigue failure under reversed large plastic strains. Hence, it is essential to find the possible shortest length of the core considering the low-cycle fatigue endurance of the steel core. To this aim, the possible minimum length (i.e., critical length) of the core was evaluated using the Coffin-Manson fracture rule (Uriz 2005) and following the methodology represented in (Hoveidae and Radpour 2021). The basic mechanical properties assumed for the steel and the SMA materials are summarized in Table 1. Furthermore, the fatigue constants for the steel material can be found in (Hoveidae and Radpour 2021).

Table 1. Basic material properties of the HSCBRB core materials

Material	E (GPa)	F_y (MPa)	Reference
Steel	191.02	373.72	(Hartloper et al. 2021)
SMA (Ni-Ti)	27.5	414	(Vafaei and Eskandari 2016)

According to the procedure specified in (Hoveidae and Radpour 2021), the geometric features of the braced frame are required to numerically evaluate the critical core length, L_c. For this purpose, the geometric characteristics of a 4-story braced frame, assumed for the evaluation of the system-level response of the proposed BRB in the following section, were adopted. To identify the efficacy of the proposed device in reducing the residual drift response of BRBFs, the system-level responses of the proposed device should be compared with that of the conventional BRBs. Therefore, two types of BRBFs incorporating the conventional BRBs and the proposed HSCBRB were considered. Using the procedure in (Hoveidae and Radpour 2021), the critical core lengths of the proposed HSCBRB are evaluated and summarized in Table 2. For the conventional BRB, which typically includes a long core without the potential for fatigue rupture, the specified critical core length in Table 2 reflects the initial core length.

Table 2. Estimated critical core lengths

BRB type	L_c (mm)
Conventional BRB	4600
HSCBRB	300

As shown in Table 2, the possible shortest core lengths, L_c, of 300 mm is adopted for the proposed HSCBRB. It is worth mentioning that due to the excellent low-cycle fatigue resistance of SMA material, the critical core length of the HSCBRB was only assessed based on the fatigue strength of the steel material. However, the evaluated critical core length was checked for the maximum recoverable strain that could be experienced by the SMA core. By taking into consideration that the maximum recoverable strain for the specified SMA material is 6% (Tazarv and Saiidi 2015), and assuming that the plastic deformations are concentrated at the brace core, the critical core length of the proposed HSCBRB inside the braced frame represented in Fig. 2 can be calculated as follows:

$$
\begin{aligned}
&\Delta_{brace}^{\max} = \Delta_{story}^{\max} \times \cos\theta \\
&\Delta_{story}^{\max} = \text{Allowable drift} \times H \\
&\Delta_{brace}^{\max} = 0.02 \times 320 \times 0.84 = 5.37 \text{ cm} \\
&\Delta_{brace}^{\max} \approx \varepsilon_{\text{recoverable}}^{SMA} \times L_c \\
&L_c = \frac{5.37}{0.06} \approx 90 \text{ cm}
\end{aligned}
\tag{1}
$$

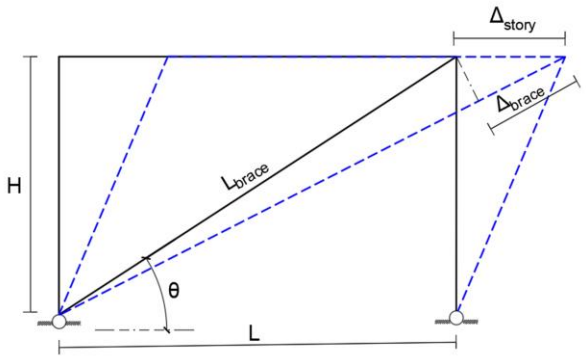


Fig. 2. Illustration of inter-story drift vs. brace axial deformation

In Eq. (1), the maximum permissible inter-story drift ratio of the braced frame was assumed as 2%, according to the Iranian code of practice for the seismic design of buildings (2014). As noted in Eq. (1), considering the story height, H, of 3.2 m and the span length, L, of 5 m for the prototype BRBFs, the critical core length of the HSCBRB, based on the maximum recoverable strain of the SMA core, was computed as 90 cm. The computed critical core length was significantly greater than the value represented in Table 2. Thus, to evaluate the system-level responses of the braced frames incorporating the proposed HSCBRBs, the core length was taken as 900 mm.

4. Characteristics of the BRB members

The present study aims to assess the seismic response of buckling-restrained braced frames equipped with SMA-based BRB members. To have an exact comparison of the seismic responses of conventional and the proposed BRBs, the BRB core areas were tuned to attain identical yielding strengths. The total brace length was set to 4600 mm, according to the geometric specifications of the designed prototype 4-story BRBF. The adjusted cross-sectional areas for BRBs are represented in Table 3. As shown in Table 3, the BRB core area for the conventional BRB is illustrated by A, whereas the areas of the core, elastic member, and the connections are represented as ratios of A. In Table 3, L_c, L_{el}, L_{con}, A_c, A_{el}, and A_{con} represent the length of the core, the length of the elastic part, the length of the connection, the BRB core area, and the total areas of the elastic part and the connections, respectively. Furthermore, A_{SMA} and A_{steel} characterize the SMA and the steel core areas in the HSCBRB, respectively. HSCBRB was designed and detailed according to the methodology proposed in (Hoveidae and Radpour, 2021). Furthermore, the ratio of the SMA and the steel core areas is assumed as 20% in this study.

Table 3. Adjustment of the geometric characteristics of the BRBs

BRB type	L_c (mm)	L_{el} (mm)	L_{con} (mm)	A_c	A_{el}	A_{con}
Conventional BRB	4600	*N.A.*	400	A	*N.A.*	$3A$
HSCBRB	900	3700	400	$A_{Steel}=0.783A$	$3A$	$3A$
				$A_{SMA}=0.195A$	$3A$	$3A$

Laboratory tests to assess the local and global responses of BRBs are desirable but naturally cost unaffordable. The alternate attractive option to capture the response of BRBs is the computer simulation that integrates realistic BRB mechanical and geometric characteristics.

5. Constitutive material model for steel

The well-known Voce-Chaboche (VC) constitutive material model is widely used in finite element packages. This material model combines the isotropic and kinematic hardening laws (Voce 1984; Chaboche et al. 1979). The initial yield stress in structural steels is typically underestimated by about 10%–30% using the classic VC metal plasticity model (Hartloper et al. 2021). To achieve a realistic response of BRBs, in this paper, the Updated Voce-Chaboche (UVC) model proposed by Hartloper et al. (2021) was adopted. The initial yield stress, as well as the initial yield

plateau response, can be well predicted by the UVC material model. Furthermore, the discontinuous yielding phenomenon in mild steels can be accurately captured by the UVC model. The calibrated material constants (AISC 341-16, 2016) for the adopted mild steel are summarized in Table 4, where E , σ_0 , C_1 , γ_1 , C_2 , γ_2 , Q_∞ , b , D_∞ and a stand for the elasticity modulus of the steel material, the initial yield stress of the steel material, the kinematic hardening parameter related to the first back-stress, the saturation rate of kinematic hardening related to the first back-stress, a kinematic hardening parameter related to the second back-stress, saturation rate of kinematic hardening related to the second back-stress, the maximum increase in yield stress due to cyclic hardening, saturation rate of Q_∞ , decrease in the initial yield stress, and saturation rate of D_∞ , respectively.

Table 4. Components of the UVC constitutive model (Hartloper et al. 2021)

Steel grade	A992-Gr50
E (GPa)	191.02
σ_0 (MPa)	373.72
C_1 (MPa)	25621
γ_1	235.12
C_2 (MPa)	942.18
γ_2	3.16
Q_∞ (MPa)	141.47
b	15.20
D_∞ (MPa)	135.95
a	211.16

6. System-level response of the HSCBRB

6.1 Design of prototype buildings

The preceding section decribed the components of the conceptual HSCBRB. Nevertheless, it is crucial to investigate and compare the seismic responses of the braced frames eqquiped with conventional and the proposed BRBs. For this purpose, 4-story and 15-story steel braced frames were considered. Assuming a typical story height of 3.2 m, the maximum number of stories for the buckling-restrained braced frame with simply supported connections permitted either by the ASCE 7-16 (2016) or the Iranian seismic code (2014) is noted as 15. Therefore, in this paper, the maximum number of stories of the study buildings is limited to 15. Fig. 3 illustrates the plan view and the elevation of the study buildings. As shown in Fig. 3, the plan of the building includes four bays of 5 m in each direction.

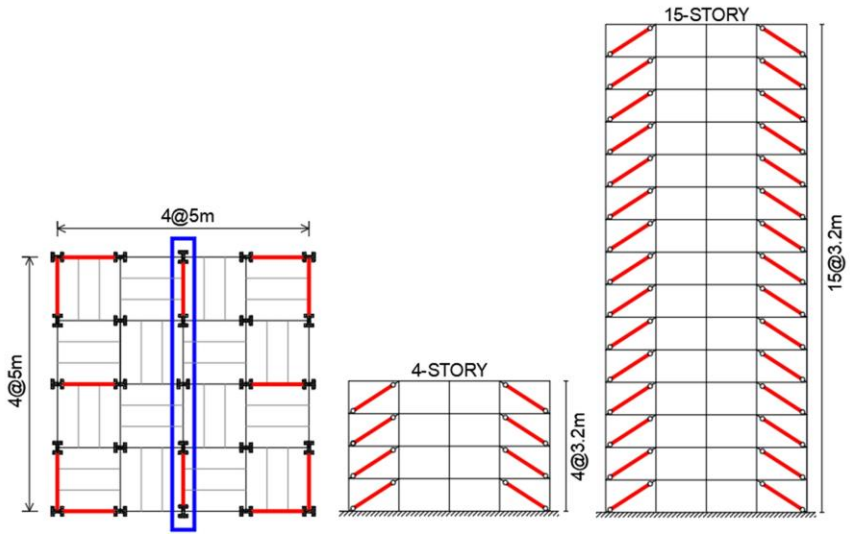


Fig. 3. Plan and elevation views of the study buildings

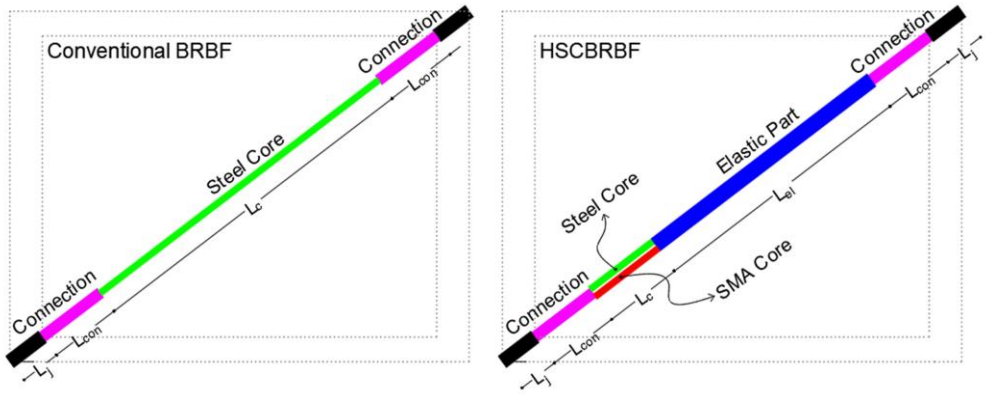


Fig. 4. Components of the BRBs inside the braced frames

The lengths and areas of the BRB components are consistent with the data provided in Table 3. The lengths of end connections and joints were specified as 400 mm and 270 mm, respectively. To have an accurate comparison between the lateral strength and stiffness of the braced frames, a detailed numerical model including the core, the end-connection, and the elastic part was adopted, as shown in Fig. 4.

The study buildings were first modeled and designed in the ETABS environment. The seismic analysis of the buildings was carried out according to the Iranian seismic code (2014). The buildings were supposed to be located in Tabriz (a very high seismic region) on type III soil. A composite steel deck floor system was assumed. All beam-column connections, as well as the brace ends, were supposed as pinned at all story levels. Furthermore, the roof and floor

loads were supposed as per Table 5. The braces were modeled using serially connected frame elements. The unbraced length ratio of the braces was assumed as a very small value to simulate the non-buckling response and to ensure the pure axial deformation of the BRBs.

Table 5. Applied gravity loads

Location	Dead load (kN/m^2)	Live load (kN/m^2)	Live partition (kN/m^2)	Snow load (kN/m^2)
Roof	4.413	1.471	0.564	1.029
Floor	3.923*	1.961	1.176	N.A.

The seismic design of the study frames was conducted according to the equivalent lateral force method (Iranian seismic code 2014). The design base shear ratios, C , of the study buildings incorporating various BRBs are summarized in Table 6. A response reduction factor $R = 7$ and an importance factor $I = 1$ were adopted for the prototype buildings. The BRB core areas were tuned to achieve equal yielding strengths. Nevertheless, owing to the application of a reduced-length core, the initial (i.e., elastic) stiffness of HSCBRBFs was higher than that of conventional BRBFs. The fundamental period, $T_{analytical}$, of the BRBFs was computed using the structural properties and deformational characteristics of the resisting elements. The fundamental period shall not exceed the product of the coefficient $C_u = 1.25$ for the upper limit on the calculated period and the empirical fundamental period, $T_{empirical}$. The empirical period depends on the building's total height, h , and is determined as $0.05h^{0.75}$ (Iranian seismic code, 2014). The governing periods are characterized by $1.25T_{empirical}$ in Table 6. Consequently, equal design base shear ratios are adopted for the buildings equipped with various BRB types, despite having various initial stiffness values. The seismic design data for the study buildings are summarized in Table 6. In addition to the code-based design, the beams and columns were designed for the adjusted maximum tension and compression forces developed in the BRBs. Table 7 summarizes the section sizes adopted for the braces, beams, and columns. Considering identical lateral strength and stiffness for the BRBFs, the same section sizes were adopted for the beams, columns, and BRBs, as shown in Table 7.

289

Table 6. Seismic data of the study buildings

BRBF		Periods			Seismic parameters		
		$T_{empirical\ (s)}$	$1.25*T_{empirical}$ (s)	$T_{analytical}$ (s)	PGA (g)	R	C
4-Story	Conventional BRBF	0.34	0.42	0.817	0.35	7	0.14
	HSCBRBF	0.34	0.42	0.635			
15-Story	Conventional BRBF	0.91	1.13	2.119	0.35	7	0.09
	HSCBRBF	0.91	1.13	1.835			

Table 7. Member sizes of the study buildings

Model	Story level	Columns	Beams	BRB core area (cm^2)
4-Story	1	W12x53	W12x19	16
	2	W12x53	W12x19	14
	3	W12x35	W12x19	12
	4	W12x35	W12x19	7
15-Story	1	W14x426	W12x19	44
	2	W14x426	W12x19	42
	3	W14x426	W12x19	42
	4	W14x342	W12x19	42
	5	W14x342	W12x19	42
	6	W14x342	W12x19	42
	7	W14x233	W12x19	42
	8	W14x233	W12x19	38
	9	W14x233	W12x19	38
	10	W14x159	W12x19	38
	11	W14x159	W12x19	38
	12	W14x159	W12x19	38
	13	W14x82	W12x19	38
	14	W14x82	W12x19	30
	15	W14x82	W12x19	20

290

291

292 **6.2. Computational modeling of the BRBFs**

293 This section designates the numerical simulation of the BRBFs. As revealed in Fig. 3, the central frame of the study
294 building was considered for two-dimensional modeling of the 4-story and 15-story braced frames in the OpenSEES
295 environment. In the numerical models, the geometric characteristics of the structural members are consistent with the
296 data provided in Table 3. A displacement-based *dispBeamColumn* element was identified for the steel core in
297 conventional BRB. Likewise, the hybrid core in the HSCBRB was modeled using two parallel *dispBeamColumn*
298 elements serially connected to the elastic member. A nonlinear force-based *forcebeamColumn* element was adopted
299 for the beams and columns. The rigid parts of the frame, end connections, and the elastic part of the HSCBRB were
300 simulated by *elasticBeamColumn* elements since they were likely to behave elastically. The brace elements were
301 defined using a fiber-based nonlinear section with an imaginary large moment of inertia. The assumed large moment
302 of inertia and subsequently large flexural rigidity of the brace components ensures the non-buckling response of the
303 BRBs. A *ZeroLength* element was used to simulate the pinned connection of the brace and beam ends. To account for

the P-Δ effects, a leaning column with a high moment of inertia was employed. A rigid truss element was used to connect the leaning column to the main frame at each story level. The inherent damping was modeled as Rayleigh damping and a critical damping ratio of 2% was adopted. The UVC constitutive material model (Hartloper et al. 2021), using the calibrated parameters summarized in Table 4, was implemented to capture the force-deformation response of the steel material.

SMAs are recently used in seismic resilience design due to their excellent superelasticity. The key characteristics of Nickle-Titanium (Ni-Ti) SMA include desirable fatigue and corrosion resistance, variety in shapes, and outstanding self-centering capacity. The characteristic flag-shaped response of Ni-Ti shape memory alloy is attributed to the transformations between the austenite and the martensite phases. In recent years, several constitutive models have been proposed for the description of the mechanical behavior of SMAs. In this paper, the *SelfCentering* constitutive model available in the OpenSEES library was adopted to simulate the superelastic response of the SMA core. This material was primarily developed to simulate a self-centering brace including a friction fuse (Christopoulos et al. 2008). However, it could potentially be used for any similar self-centering material like the SMA that exhibits an idealized flag-shaped hysteretic response. The required parameters for modeling the stress-strain response of an SMA material using this material model are illustrated in Fig. 5, where f_y reflects the austenite yield strength. k_1 and k_2 characterize the austenite modulus and the post-yield stiffness, respectively. In addition, α and β symbolize the secondary post-yield stiffness ratio and the lower plateau stress factor, respectively. The strains at the end of the austenite-to-martensite phase transformation and the ultimate strains at fracture are represented by ε_s and ε_u, correspondingly. This material model has been validated and implemented by several scholars (Vafaei and Eskandari 2016; Tazarv and Saiidi 2015) to simulate the flag-shaped response of SMA in the OpenSEES. The calibrated parameters are summarized in Table 8. The assumed parameters are comparable with those used in the component-level study of the BRBs in section 4. A rigid diaphragm using *equalDOF* command was assumed at the story levels. Fig. 6 represents the detailed finite element model of the BRBFs created in the OpenSEES.

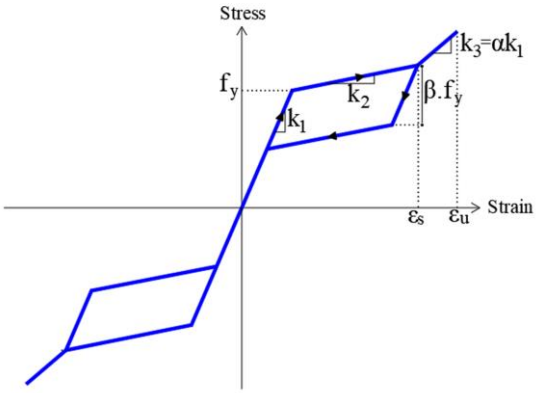


Fig. 5. Idealized nonlinear strain-stress relationship for the SMA material (Tazarv and Saiidi 2015)

Table 8. Mechanical properties of the SMA material (Tazarv and Saiidi 2015)

k_1 (MPa)	k_2 (MPa)	f_y (MPa)	β	ε_s (%)	α
27579	3882	414	0.39	5.5	0.58

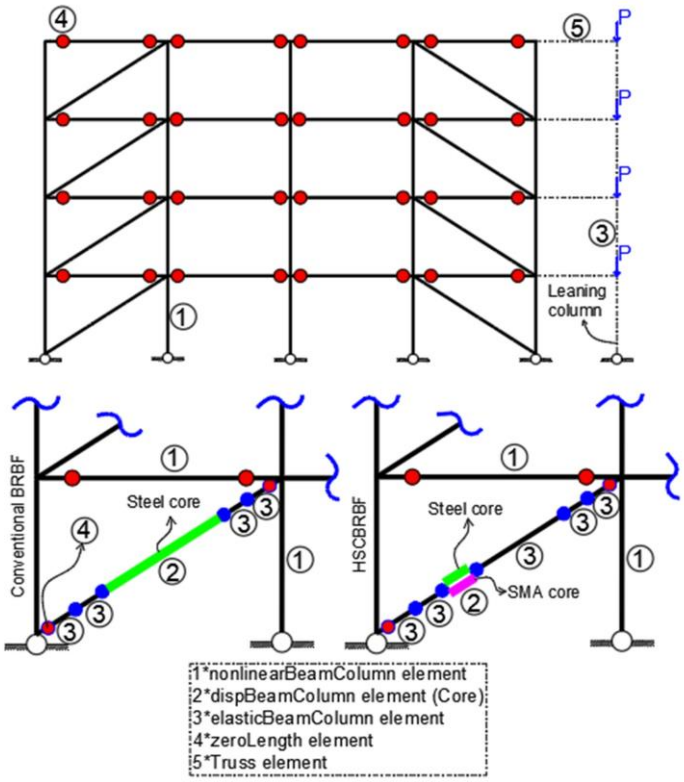


Fig. 6. Two-dimensional OpenSEES model of BRBFs

6.3. Nonlinear static pushover analysis

Nonlinear static pushover analysis was conducted to evaluate the monotonic response and quantitatively compare the post-elastic stiffness of the conventional BRBFs and HSCBRBFs. The lateral force distribution was supposed to follow the first mode shape. The two-dimensional braced frames were pushed up to the target displacement corresponding to 2% of the total frame height and consequently the response of the braced frames in terms of the roof displacement versus the base shear was captured. The pushover response curves are represented in Fig. 7.

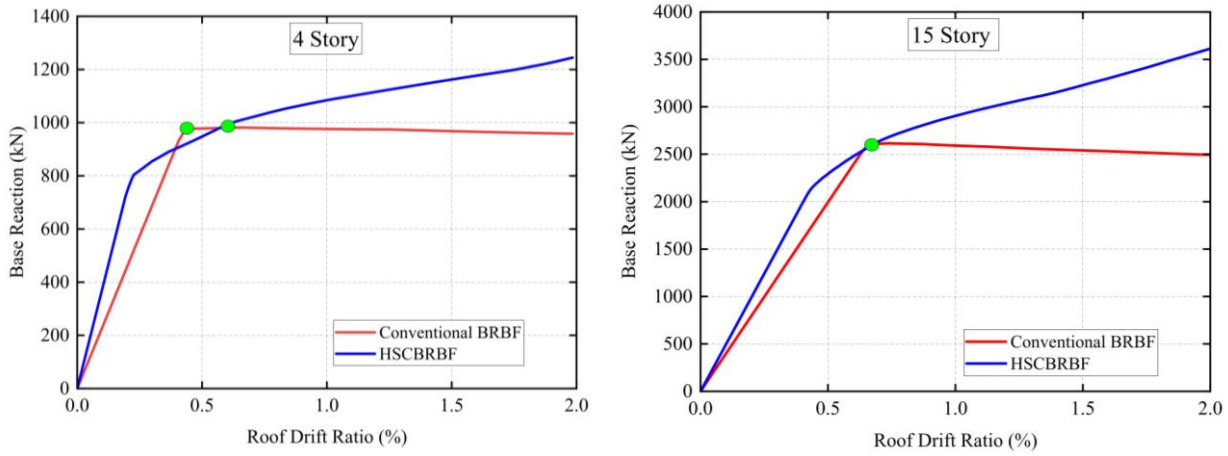


Fig. 7. Pushover response curves for the study BRBFs

As shown in Fig. 7, the 4-story and 15-story BRBFs exhibit equal yielding strengths since identical yielding strengths are adopted for the BRBs, as discussed in section 4. The yielding strengths for the 4-story and 15-story BRBFs are noted as 1000 kN and 2700 kN, respectively. In addition, the HSCBRBFs exhibits smaller first-yielding displacements compared with conventional BRBFs, which can lead to higher ductility of the HSCBRBFs. This phenomenon can be attributed to the smaller cross-sectional area of the steel core employed in the HSCBRBs compared with that of conventional BRBs. As expected, the HSCBRBFs exhibit higher post-elastic stiffness ratios than the conventional BRBFs. As shown in Fig. 7, the HSCBRBF shows a tri-linear lateral response curve, whereas a bi-linear response curve is observed for the conventional BRBF. The high strain-hardening of the reduced-length cores in the proposed HSCBRBs increases the post-elastic stiffness of the BRBFs, as shown in Fig. 7. In contrast, the capacity curve of the conventional BRBF can be designated by a degrading slope, which follows a very short plateau. Such a degrading pushover response for the conventional BRBFs can be attributed to the application of the UVC material model for the steel core and the P-Δ effects. A similar degrading pushover response for the conventional BRBFs was reported by

Atlayan and Charney (2014). In summary, the buckling-restrained braced frames equipped with the proposed HSCBRBs show significantly higher post-elastic stiffness ratios than the conventional BRBFs.

6.4. Seismic analysis

6.4.1. Selection of ground motion records

Nonlinear dynamic analysis is an efficient method to evaluate the seismic behavior of buildings against earthquakes. Both record selection and scaling are important stages for the accurate derivation of seismic response through dynamic analysis. The ASCE 7-16 (2016) and the Iranian seismic code (2014) regulations recommend the selection of at least eleven and seven ground motion records, respectively, to conduct a time history analysis. Furthermore, it is recommended to select a suite of ground motion records that are consistent with the site-specific likely earthquakes. In this paper, a set of twenty-two far-field ground motion records recommended by the FEMA-P695 (2009) was considered for the dynamic analysis of the study frames. Table 9 summarizes the record characteristics in detail. The site class data of the selected record set closely matches the site class of the designed study frames. It is noteworthy that the greatest component of the seismic events was considered for seismic analysis.

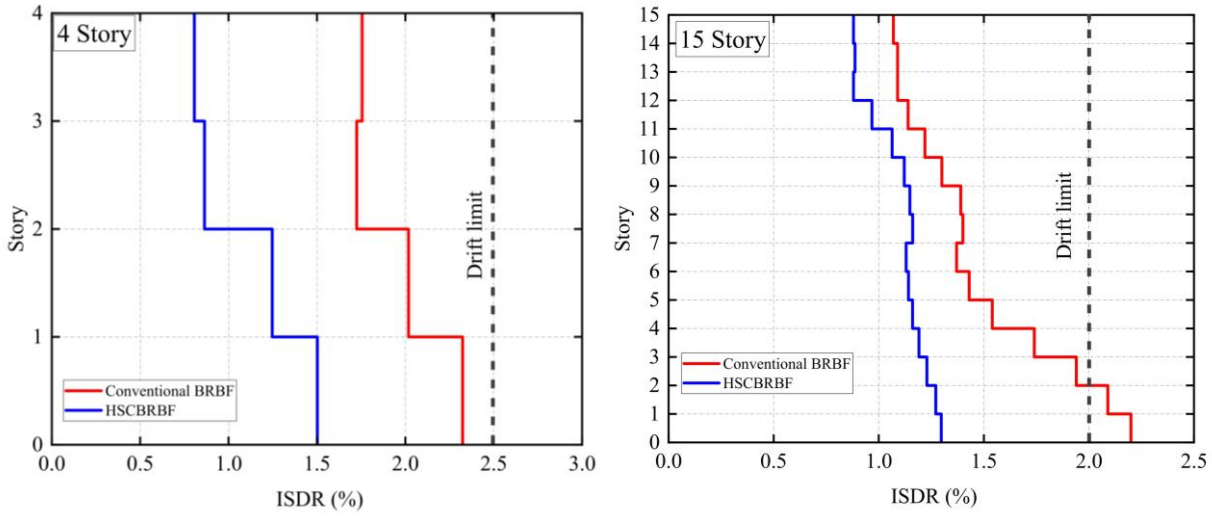
Table 9. Details of the selected ground motion records (FEMA-P695, 2009)

Record No.	Magnitude (M_w)	Year	Event Name	PGA (g)	PGV (cm/s)
1	6.7	1994	Northridge	0.52	63
2	6.7	1994	Northridge	0.48	45
3	7.1	1999	Duzce, Turkey	0.82	62
4	7.1	1999	Hector Mine	0.34	42
5	6.5	1979	Imperial Valley	0.35	33
6	6.5	1979	Imperial Valley	0.38	42
7	6.9	1995	Kobe, Japan	0.51	37
8	6.9	1995	Kobe, Japan	0.24	38
9	7.5	1999	Kocaeli, Turkey	0.36	59
10	7.5	1999	Kocaeli, Turkey	0.22	40
11	7.3	1992	Landers	0.24	52
12	7.3	1992	Landers	0.42	42
13	6.9	1989	Loma Prieta	0.53	35
14	6.9	1989	Loma Prieta	0.56	45
15	7.4	1990	Manjil, Iran	0.51	54
16	6.5	1987	Superstition Hills	0.36	46
17	6.5	1987	Superstition Hills	0.45	36
18	7	1992	Cape Mendocino	0.55	44
19	7.6	1999	Chi-Chi, Taiwan	0.44	115
20	7.6	1999	Chi-Chi, Taiwan	0.51	39
21	6.6	1971	San Fernando	0.21	19
22	6.5	1976	Friuli, Italy	0.35	31

6.4.2. Time history analysis

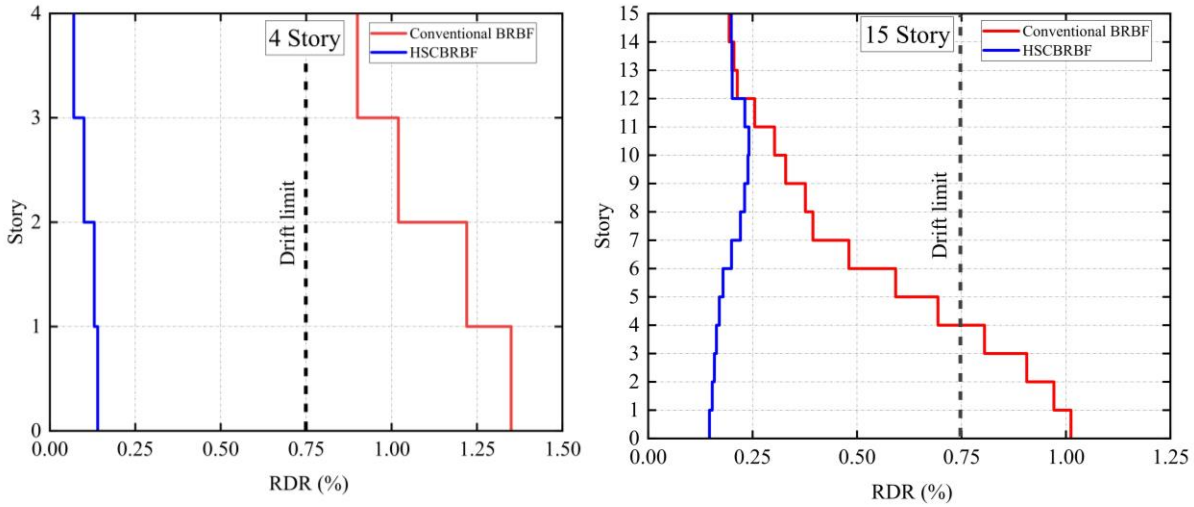
Nonlinear dynamic analyses were performed and several key characteristics of the response including the maximum Inter-Story Drift Ratio (ISDR) and the Residual Drift Ratio (RDR) of the 4-story and 15-story study frames were demonstrated. The drift ratio reflects the inter-story or the residual drift of a story divided by the story height. The mean inter-story and residual drift responses of the study frames, are illustrated in Figs. 8 and 9, respectively. Furthermore, Table 10 summarizes the mean ISDR and RDR responses under the selected earthquake set. As shown in Fig. 8 and summarized in Table 10, the maximum value of the mean ISDR responses of the 4-story conventional BRBFs is noted as 2.32%, which is below the permissible drift value of 2.5% under design basis earthquake hazard (Iranian seismic code 2014). Nevertheless, the 15-story conventional BRBF shows a maximum ISDR value of 2.2%, which marginally exceeds the allowable drift values (i.e., 2%) (Iranian seismic code 2014) in the first and the second stories.

As revealed in Fig. 8, the HSCBRBs exhibit significantly lower ISDR values compared with the conventional BRBFs. The peak values of the mean ISDR response of HSCBRBFs fall below the limiting drift value, as shown in Fig. 8. The high initial (i.e., elastic) stiffness of the short-length core accounts for the lower ISDR responses of HSCBRBFs compared with the conventional BRBFs. Fig. 9 displays the mean RDR response of the study frames under the selected far-field ground motion records. The peak values of the mean RDR response of the 4-story and 15-story conventional BRBFs are noted as 1.35%, and 1.01%, respectively, which exceed the allowable residual drift value of 0.75% recommended in the literature (Erochko et al. 2011). In contrast, the HSCBRBFs exhibits a significantly smaller RDR response. The peak values of the RDR response of the 4-story and 15-story HSCBRBFs are noted as 0.14% and 0.24%. As shown in Fig. 9 further reduction in the residual drift response is observed for the HSCBRBFs due to the self-centering potential of the SMA core. Table 10 summarizes the reduction in peak ISDR and RDR responses of the HSCBRBFs compared with the conventional BRBFs. As represented in Table 10, in comparison to the conventional BRBF, the reductions in the peak RDR response of the 4-story and 15-story HSCBRBFs are remarked as 90% and 76%, respectively. As a result, the proposed HSCBRB, which benefits the combined hysteretic response of the steel core and the flag-shaped self-centering response of the SMA core, significantly reduces the residual drift response of the braced frame. In summary, the HSCBRBs may suggest a new solution to moderate the excessive residual drifts in conventional BRBFs. In addition to the attractive re-centering capacity of the HSCBRBs, the fabrication, installation, and replacement of a short-length core seem to be easier compared with conventional BRBs.



399

400 **Fig. 8**. Comparison of the mean inter-story drift response



401

402 **Fig. 9**. Comparison of the mean residual drift response

403

Table 10. Summarized peak ISDR and RDR responses of the study frames

BRBF type		$ISDR_{max}$ (%)	RDR_{max} (%)	ISDR reduction (%)	RDR reduction (%)
4-Story	Conventional BRBF	2.32	1.35	*	*
	HSCBRBF	1.5	0.14	35	90
15-Story	Conventional BRBF	2.2	1.01	*	*
	HSCBRBF	1.3	0.24	41	76

404

6.4.3. Incremental Dynamic Analysis (IDA)

Incremental Dynamic Analysis (IDA) includes a large number of nonlinear dynamic analyses under a set of earthquake ground motions. In this method, the desired structure is subjected to dynamic analyses under several seismic excitations and the maximum response of the structure is recorded. In this paper, the maximum inter-story drift (ISDR) is chosen as the damage measure parameter (DM), which is supposed as 2.5% for 4-story BRBFs and 2% for 15-story BRBFs, as per Iranian seismic code 2014. Subsequently, spectral acceleration (Sa) of the first mode is selected as the intensity measure parameter (IM). Twenty-two far-field ground motion records suggested by ATC-63 (2008) and summarized in Table 9 were utilized in the IDA analysis. Fig. 10 represents the IDA curves for the study BRBFs, including conventional BRBF and HSCBRBF. As shown in Fig. 10, the HSCBRBFs are able to withstand larger Sa values than the conventional BRBFs. The derived IDA curves are directly used to generate the fragility curves as well as the response modification factor of the steel braced frames in the following section.

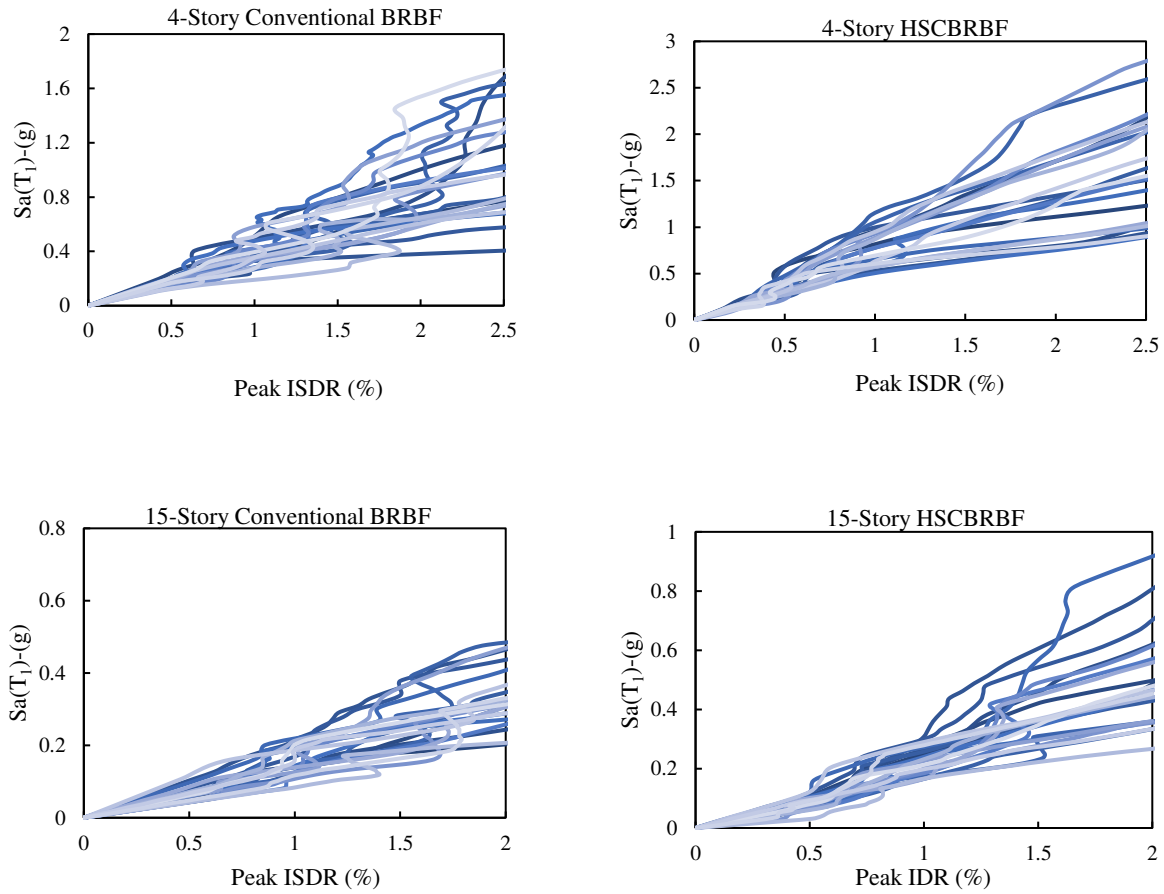


Fig. 10. IDA curves for the study BRBFs

6.4.5. Fragility response

In order to quantitatively express the vulnerability of various structural or non-structural components according to the intensity measure (IM) parameters of an earthquake, the probability of occurrence or exceeding a certain level of damage can be expressed in terms of a parameter representative of IM, such as the spectral acceleration of the first mode of the structure, the maximum acceleration or the maximum speed of the ground motion. Fragility curves are drawn using sorted values for the IM of earthquakes corresponding to the considered limit states for all ground motion records examined in IDA. In a typical fragility curve, the horizontal axis represents the desired seismic IM (spectral acceleration of the first mode of the structure) and the vertical axis represents the probability of seismic damage exceeding the desired performance level (Collapse prevention here). The normal distribution function is defined for drawing fragility curves as in the following:

$$P(C|IM = x) = \phi\left(\frac{\ln(x/\theta)}{\beta}\right)$$

$$\ln\hat{\theta} = \frac{1}{n}\sum_{i=1}^{n}\ln IM_i \tag{2}$$

$$\hat{\beta} = \sqrt{\frac{1}{n-1}\sum_{i=1}^{n}(\ln(IM_i/\hat{\theta}))^2}$$

Where x denotes the collapse spectral acceleration for each record and θ reflects the average collapse acceleration, which is equal to the average of x. Furthermore, β stands for the standard deviation of natural logarithm values. Fig. 11 represents fragility curves of the study BRBFs.

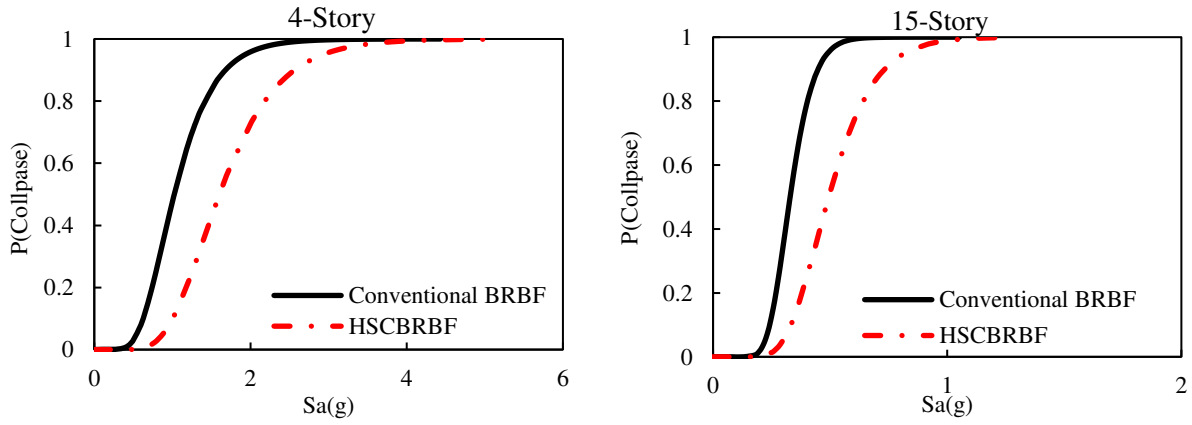


Fig 11. Fragility curves for the study BRBFs

According to Fig. 11, the probability of collapse for the 4-story conventional BRBF for a specific ground motion intensity is significantly higher compared with the 4-story HSCBRBF. Furthermore, the 15-story HSCBRBF exhibits less vulnerability in comparison to conventional BRBFs, as shown in Fig. 11. As a results, the application of SMA-based hybrid core results in less seismic vulnerability of buckling-restrained braced frames.

6.4.6. Response modification factor (R)

The response modification factor, R enables the engineers to apply the inelastic behavior of the structure without implementing a complicated nonlinear analysis in design of structures. Response modification factor is generally related to the strength, over-strength, ductility and damping characteristics of a structure. Several methods have been proposed to quantify the response modification factor. In this paper, the response modification factors of the study BRBFs are evaluated by the IDA analysis. According to the research conducted by Asgarian et al. (2021), the equation (3) can be used to evaluate the response modification factor, as in the following:

$$R = \frac{V_e}{V_s} = \frac{V_e}{V_y} \times \frac{V_y}{V_s} = R_\mu \times R_s \tag{3}$$

Where R_μ reflects the strength reduction factor due to ductility and R_s represents the over strength factor that accounts for the reserved strength of structures. The term V_y represents the maximum base shear corresponding to collapse prevention limit state of the structure. Furthermore, V_s reflects the maximum base shear corresponding to the first plastic hinge. By assuming elastic material properties and conducting linear dynamic analysis under the ground motion scale corresponding to the collapse prevention limit state of the structure, the maximum linear base shear V_e was calculated and finally the response modification factor was evaluated through equation (3). The response modification factors are calculated and summarized in Tables 11 and 12. Furthermore, the average response modification factors are represented in Table 13. According to Table 13, the average R factor for the conventional BRBFs and HSCBRBFs are noted as 5.42 and 8.53, respectively. The higher response modification factor of the proposed HSCBRBFs can be associated to the higher ductility and over-strength of the BRBs. In summary and based on the results obtained, the proposed HSCBRBF possess significantly higher response modification factor compared with conventional BRBFs. Furthermore, according to the fragility curves represented in Fig. 11, in contrast to the conventional BRBs, the

proposed HSCBRB device can significantly reduce the seismic collapse probability of steel buckling-restrained braced frames and can be considered as an efficient alternative for the conventional BRBs.

Table 11. R factor parameters of 4-Story BRBFs

	4-Story Conventional BRBF						4-Story HSCBRBF					
Record	V_y (kN)	V_s(kN)	V_e(kN)	R_s	R_μ	R	V_y(kN)	V_s(kN)	V_e(kN)	R_s	R_μ	R
1	1073	975	4879	4.5	1.1	5	1630	997	7669	4.7	1.6	7.7
2	1151	975	5117	4.4	1.2	5.2	1508	997	10813	7.2	1.5	10.8
3	1161	975	7237	6.2	1.2	7.4	1427	997	4543	3.2	1.4	4.6
4	1100	975	2794	2.5	1.1	2.8	1520	997	4339	2.8	1.5	4.3
5	1220	975	4239	3.5	1.2	4.3	1625	997	6528	4	1.6	6.5
6	1058	975	4133	3.9	1.1	4.2	1643	997	10465	6.4	1.6	10.5
7	1483	975	7338	4.9	1.5	7.5	1587	997	16554	10.4	1.6	16.6
8	1138	975	6420	5.6	1.2	6.6	1533	997	10230	6.7	1.5	10.3
9	1177	975	3613	3.06	1.2	3.7	1514	997	4496	2.9	1.5	4.5
10	1187	975	10018	8.4	1.2	10.3	1590	997	7010	4.4	1.6	7
11	1167	975	4258	3.6	1.2	4.4	1472	997	5111	3.5	1.5	5.1
12	1118	975	7080	6.3	1.1	7.3	1455	997	7038	4.8	1.5	7.1
13	1294	975	8930	6.9	1.3	9.1	1535	997	11402	7.4	1.5	11.4
14	1112	975	5290	4.7	1.1	5.4	1706	997	17283	10.1	1.7	17.3
15	1222	975	7538	6.2	1.2	7.7	1466	997	13905	9.5	1.5	13.9
16	1076	975	3861	3.6	1.1	3.9	1477	997	5471	3.7	1.5	5.5
17	1071	975	4503	4.2	1.1	4.6	1464	997	9553	6.5	1.5	9.6
18	1237	975	4236	3.4	1.3	4.3	1604	997	9774	6.1	1.6	9.8
19	1101	975	4427	4	1.1	4.5	1584	997	4703	2.9	1.5	4.7
20	1173	975	9601	8.2	1.2	9.8	1529	997	11434	7.5	1.5	11.5
21	1235	975	6589	5.3	1.3	6.7	1527	997	5757	3.8	1.5	5.7
22	1307	975	6888	5.3	1.3	7.1	1666	997	7085	4.2	1.7	7.1

Table 12. R factor parameters of 15-Story BRBFs

	15-Story Conventional BRBF						15-Story HSCBRBF					
Record	V_y(kN)	V_s(kN)	V_e(kN)	R_s	R_μ	R	V_y(kN)	V_s(kN)	V_e(kN)	R_s	R_μ	R
1	3078	2532	10031	3.3	1.2	3.9	3531	2611	31204	8.8	1.3	11.9
2	3928	2532	17666	4.5	1.5	6.9	4527	2611	22286	4.9	1.7	8.5
3	3221	2532	8188	2.5	1.3	3.2	3942	2611	19460	4.9	1.5	7.4
4	3024	2532	9824	3.2	1.2	3.9	3909	2611	37293	9.5	1.5	14.3
5	3083	2532	12250	3.9	1.2	4.8	4129	2611	18802	4.5	1.6	7.2
6	3353	2532	11750	3.5	1.3	4.6	4215	2611	21085	5	1.6	8.1
7	3460	2532	16743	4.8	1.3	6.6	4300	2611	26834	6.2	1.6	10.3
8	3336	2532	19502	5.8	1.3	7.7	4109	2611	12914	3.1	1.6	4.9
9	3131	2532	10007	3.2	1.2	3.9	3692	2611	23748	6.4	1.4	9.1
10	3404	2532	8975	2.6	1.3	3.5	4259	2611	18069	4.2	1.6	6.9
11	3020	2532	7319	2.4	1.2	2.9	3398	2611	9375	2.8	1.3	3.6
12	3372	2532	13723	4.1	1.3	5.4	4063	2611	23502	5.8	1.6	9
13	3356	2532	15893	4.7	1.3	6.3	4678	2611	25916	5.5	1.8	9.9
14	3622	2532	15346	4.2	1.4	6.1	4446	2611	32842	7.4	1.7	12.6
15	3626	2532	18737	5.2	1.4	7.4	3979	2611	12396	3.1	1.5	4.7
16	2902	2532	10317	3.6	1.1	4.1	3782	2611	22234	5.9	1.4	8.5
17	3221	2532	10665	3.3	1.3	4.2	3961	2611	21377	5.4	1.5	8.2
18	3509	2532	9715	2.8	1.4	3.8	4347	2611	27401	6.3	1.7	10.5
19	3057	2532	8670	2.8	1.2	3.4	3973	2611	11617	2.9	1.5	4.4
20	3080	2532	11940	3.9	1.2	4.7	4122	2611	20061	4.9	1.6	7.7
21	3438	2532	6987	2	1.4	2.8	3535	2611	9282	2.6	1.3	3.5
22	3586	2532	15465	4.3	1.4	6.1	3997	2611	32063	8	1.5	12.3

Table 13. Average R values

BRBF	R
Conventional BRBF	5.4
HSCBRBF	8.5

Summary and conclusion

This paper introduces a novel SMA-based BRB. Nonlinear time history analysis is conducted and the seismic responses in terms of maximum and residual drifts are reported. Furthermore, by conducting incremental dynamic analyses (IDA), the fragility response and response modification factors of the buckling-restrained braced frames incorporating the conventional and the proposed BRBs are evaluated. The results of this study are summarized in the following:

- The pushover analysis of the BRBFs equipped with the proposed HSCBRB and the conventional BRBs demonstrates that the HSCBRBs provide higher post-elastic stiffness than the conventional BRBs. While the pushover response of the conventional BRBFs is characterized by a softening response due to P-Δ effects, the HSCBRBFs exhibit a hardening response with a positive post-yielding stiffness.

- Nonlinear dynamic analysis designates that the proposed HSCBRB decreases the ISDR and specifically the RDR responses of the buckling-restrained braced frames. Compared with conventional BRBFs, the peak ISDR responses of the 4-story and 15-story HSCBRBFs are reduced by 35% and 41%, respectively. The corresponding reductions in the mean RDR responses are noted as 97% and 83%, respectively.
- According to the fragility curves derived from IDA analysis, the probability of collapse for the conventional BRBFs is significantly higher compared with HSCBRBFs.
- The recommended response modification factors for design of conventional BRBFs and the proposed HSCBRBFs are obtained as 5.4, and 8.5 respectively. The response modification factor of 5.42 obtained for conventional BRBFs is lower than the value 8 recommended by ASCE 7-16 for buckling-restrained braced frames. Finally, the proposed HSCBRBs provide an outstanding self-centering capacity for the steel buckling-restrained braced frames. Furthermore, the higher response modification factor of HSCBRBFs compared with conventional BRBFs results in lower base shear values for design of steel buckling-restrained braced frames.

Statements and Declarations

Funding
The authors declare that no funds, grants, or other support were received during the preparation of this manuscript.

Competing Interests
The authors have no relevant financial or non-financial interests to disclose.

Data Availability
The datasets generated during and/or analyzed during the current study are available from the corresponding author on reasonable request.

Declaration of interests
☒ The authors declare that they have no known competing financial interests or personal relationships that could have appeared to influence the work reported in this paper.
☐ The authors declare the following financial interests/personal relationships which may be considered as potential competing interests:

References

AISC 341-16 (2016). (American Institute of Steel Construction), Seismic Provisions for Structural Steel Buildings, Chicago, IL.

American Society of Civil Engineers (ASCE). Structural engineering institute (SEI), minimum design loads for buildings and other structures. (2016). American Society of Civil Engineers/Structural Engineering Institute, Reston.

Applied Technology Council. (2009). Quantification of building seismic performance factors. US Department of Homeland Security, FEMA.

Asgarian, B., & Moradi, S. (2011). Seismic response of steel braced frames with shape memory alloy braces. Journal of Constructional Steel Research, 67(1), 65-74.

Asgarian, B., Jamalian, A., & Jalaeefar, A. (2021). Response Modification Factor of Steel Braced Frames Equipped with Smart Hybrid Re-Centering Device. International Journal of Steel Structures, 21, 2004-2017.

Atlayan, O., & Charney, F. A. (2014). Hybrid buckling-restrained braced frames. Journal of Constructional Steel Research, 96, 95-105.

Avci-Karatas, C., Celik, O. C., & Yalcin, C. (2018). Experimental investigation of aluminum alloy and steel core buckling restrained braces (BRBs). International Journal of Steel Structures, 18, 650-673.

Bazzaz, M., Andalib, Z., Kheyroddin, A., & Kafi, M. A. (2015). Numerical comparison of the seismic performance of steel rings in off-centre bracing system and diagonal bracing system. Journal of Steel and Composite Structures, 19(4), 917-937.

Bazzurro, P., & Cornell, C. A. (1994). Seismic hazard analysis of nonlinear structures. II: Applications. Journal of Structural Engineering, 120(11), 3345-3365.

Black, C., Aiken, I. D., & Makris, N. (2002). Component testing, stability analysis, and characterization of buckling-restrained unbonded braces (TM). Pacific Earthquake Engineering Research Center.

Chaboche, J. L., Van, K. D., & Cordier, G. (1979). Modelization of the strain memory effect on the cyclic hardening of 316 stainless steel.

Christopoulos, C., Tremblay, R., Kim, H. J., & Lacerte, M. (2008). Self-centering energy dissipative bracing system for the seismic resistance of structures: development and validation. Journal of structural engineering, 134(1), 96-107.

DesRoches, R., McCormick, J., & Delemont, M. (2004). Cyclic properties of superelastic shape memory alloy wires and bars. Journal of Structural Engineering, 130(1), 38-46.

Dong, H., Du, X., & Han, Q. (2019). Seismic responses of steel frame structures with self-centering energy dissipation braced on shape memory alloy cables. Advances in Structural Engineering, 22(9), 2136-2148.

Eatherton, M. R., Fahnestock, L. A., & Miller, D. J. (2014). Computational study of self-centering buckling-restrained braced frame seismic performance. Earthquake engineering & structural dynamics, 43(13), 1897-1914.

Erochko, J., Christopoulos, C., Tremblay, R., & Choi, H. (2011). Residual drift response of SMRFs and BRB frames in steel buildings designed according to ASCE 7-05. Journal of Structural Engineering, 137(5), 589-599.

Fahnestock, L. A., Sause, R., Ricles, J. M., & Lu, L. W. (2003). Ductility demands on buckling-restrained braced frames under earthquake loading. Earthquake Engineering and Engineering Vibration, 2, 255-268.

Fang, C., Wang, W., Ricles, J., Yang, X., Zhong, Q., Sause, R., & Chen, Y. (2018). Application of an innovative SMA ring spring system for self-centering steel frames subject to seismic conditions. Journal of Structural Engineering, 144(8), 04018114.

Ghassemieh, M., & Kargarmoakhar, R. (2013). Response modification factor of steel frames utilizing shape memory alloys. Journal of intelligent material systems and structures, 24(10), 1213-1225.

Ghowsi, A. F., & Sahoo, D. R. (2020). Near-field earthquake performance of SC-BRBs with optimal design parameters of SMA. Journal of Constructional Steel Research, 175, 106321.

Ghowsi, A. F., Sahoo, D. R., & Kumar, P. A. (2020). Cyclic tests on hybrid buckling-restrained braces with Fe-based SMA core elements. Journal of Constructional Steel Research, 175, 106323.

Ghowsi, A. F., & Sahoo, D. R. (2020). Seismic response of SMA-based self-centering buckling-restrained braced frames under near-fault ground motions. Soil Dynamics and Earthquake Engineering, 139, 106397.

Hakim, S. J. S., Noorzaei, J., Jaafar, M. S., Jameel, M., & Mohammadhassani, M. (2011). Application of artificial neural networks to predict compressive strength of high strength concrete. Int. J. Phys. Sci, 6(5), 975-981.

Hartloper, A. R., de Castro e Sousa, A., & Lignos, D. G. (2021). Constitutive modeling of structural steels: nonlinear isotropic/kinematic hardening material model and its calibration. Journal of Structural Engineering, 147(4), 04021031.

Hashemi, S. V., Pouraminian, M., Sadeghi, A., & Pourbakhshian, S. (2021). Seismic Performance of Buckling Restrained Braced Frames with Shape Memory Alloy Subjected to Mainshock-Aftershock Near-Fault Ground Motion. Modares Civil Engineering journal, 21(4), 35-50.

Hoveidae, N., Tremblay, R., Rafezy, B., & Davaran, A. (2015). Numerical investigation of seismic behavior of short-core all-steel buckling restrained braces. Journal of Constructional Steel Research, 114, 89-99.

Hoveidae, N. (2019). Multi-material core as self-centering mechanism for buildings incorporating BRBs. Earthquakes and Structures, 16(5), 589.

Hoveidae, N., & Radpour, S. (2021). A novel all-steel buckling restrained brace for seismic drift mitigation of steel frames. Bulletin of Earthquake Engineering, 19, 1537-1567.

Hu, B., Min, Y., Wang, C., Xu, Q., & Keleta, Y. (2022). Design, analysis and application of the double-stage yield buckling restrained brace. Journal of Building Engineering, 48, 103980.

Iranian Code of Practice for Seismic Resistant Design of Buildings, Standard No. 2800, 4th Edition building and housing research center. (2014). Tehran, Iran.

Kalkan, E., & Chopra, A. K. (2010). Practical guidelines to select and scale earthquake records for nonlinear response history analysis of structures.

Kazemi, F., & Jankowski, R. (2023). Seismic performance evaluation of steel buckling-restrained braced frames including SMA materials. Journal of Constructional Steel Research, 201, 107750.

Ke, K., & Chen, Y. (2016). Seismic performance of MRFs with high strength steel main frames and EDBs. Journal of Constructional Steel Research, 126, 214-228.

Ke, K., Zhou, X., Zhu, M., Yam, M. C., Wang, Y., & Zhang, H. (2022). Seismic evaluation of industrial steel moment resisting frames with shape memory alloys using performance-spectra-based method. Journal of Building Engineering, 48, 103950.

Kiggins, S., & Uang, C. M. (2006). Reducing residual drift of buckling-restrained braced frames as a dual system. Engineering Structures, 28(11), 1525-1532.

Khorami, M., Alvansazyazdi, M., Shariati, M., Zandi, Y., Jalali, A., & Tahir, M. (2017). Seismic performance evaluation of buckling restrained braced frames (BRBF) using incremental nonlinear dynamic analysis method (IDA).

Kim, J., & Choi, H. (2004). Behavior and design of structures with buckling-restrained braces. Engineering structures, 26(6), 693-706.

Luco, N., & Cornell, C. A. (1998, May). Effects of random connection fractures on the demands and reliability for a 3-story pre-Northridge SMRF structure. In Proceedings of the 6th US national conference on earthquake engineering (Vol. 244, pp. 1-12). El Cerrito, CA, USA: EERI.

Luco, N., & Cornell, C. A. (2000). Effects of connection fractures on SMRF seismic drift demands. Journal of Structural Engineering, 126(1), 127-136.

Mehanny, S. S. F. (2000). Modeling and assessment of seismic performance of composite frames with reinforced concrete columns and steel beams. Stanford University.

Miller, D. J., Fahnestock, L. A., & Eatherton, M. R. (2012). Development and experimental validation of a nickel–titanium shape memory alloy self-centering buckling-restrained brace. Engineering Structures, 40, 288-298.

Mohammadhassani, M., Jumaat, M. Z., & Jameel, M. (2012). Experimental investigation to compare the modulus of rupture in high strength self compacting concrete deep beams and high strength concrete normal beams. Construction and Building Materials, 30, 265-273.

Moradi, S., Alam, M. S., & Asgarian, B. (2014). Incremental dynamic analysis of steel frames equipped with NiTi shape memory alloy braces. The Structural Design of Tall and Special Buildings, 23(18), 1406-1425.

Nassar, A. A. (1991). Seismic demands for SDOF and MDOF systems. Stanford University.

Nazarimofrad, E., & Shokrgozar, A. (2019). Seismic performance of steel braced frames with self-centering buckling-restrained brace utilizing superelastic shape memory alloys. The Structural Design of Tall and Special Buildings, 28(16), e1666.

Pandikkadavath, M. S., & Sahoo, D. R. (2016). Analytical investigation on cyclic response of buckling-restrained braces with short yielding core segments. International Journal of Steel Structures, 16, 1273-1285.

Pister, K. S. (1980). Structural Engineering and Structural Mechanics: A Volume Honoring Egor P. Popov. Prentice-Hall.

Prinz, G. S., & Richards, P. W. (2012). Seismic performance of buckling-restrained braced frames with eccentric configurations. Journal of Structural Engineering, 138(3), 345-353.

Qiu, C., & Du, X. (2020). Seismic performance of multistory CBFs with novel recentering energy dissipative braces. Journal of Constructional Steel Research, 168, 105864.

Qiu, C., Fang, C., Liang, D., Du, X., & Yam, M. C. (2020). Behavior and application of self-centering dampers equipped with buckling-restrained SMA bars. Smart Materials and Structures, 29(3), 035009.

Rahgozar, N., & Alam, M. S. (2023). Seismic collapse assessment of hybrid self-centering piston-based braced frames equipped with SMA bars and friction springs. Journal of Constructional Steel Research, 208, 108003.

Sabelli, R., Mahin, S., & Chang, C. (2003). Seismic demands on steel braced frame buildings with buckling-restrained braces. Engineering structures, 25(5), 655-666.

Seismosoft, SeismoMatch. (2022) A computer program for spectrum matching of earthquake records. https://www.seismosoft.com

Shams, A. S., & Ghobadi, M. S. (2021). Development of a high-performance hybrid self-centering building for seismic resilience. Engineering Structures, 226, 111382.

Tazarv, M., & Saiid Saiidi, M. (2015). Reinforcing NiTi superelastic SMA for concrete structures. Journal of Structural Engineering, 141(8), 04014197.

Tian, L., & Qiu, C. (2018). Controlling residual drift in BRBFs by combining SCCBFs in parallel. Journal of performance of constructed facilities, 32(4), 04018047.

Tremblay, R., Bolduc, P., Neville, R., & DeVall, R. (2006). Seismic testing and performance of buckling-restrained bracing systems. Canadian Journal of Civil Engineering, 33(2), 183-198.

Uriz, P. (2005). Towards earthquake resistant design of concentrically braced steel structures. University of California, Berkeley.

Vafaei, D., & Eskandari, R. (2016). Seismic performance of steel mega braced frames equipped with shape-memory alloy braces under near-fault earthquakes. The Structural Design of Tall and Special Buildings, 25(1), 3-21.

Voce, E. (1948). The relationship between stress and strain for homogeneous deformation. Journal of the Institute of Metals, 74, 537-562.

Wang, H., Nie, X., & Pan, P. (2017). Development of a self-centering buckling restrained brace using cross-anchored pre-stressed steel strands. Journal of Constructional Steel Research, 138, 621-632.

Wang, B., & Zhu, S. (2018). Cyclic tension–compression behavior of superelastic shape memory alloy bars with buckling-restrained devices. Construction and Building Materials, 186, 103-113.

Watanabe, A., Hitomi, Y., Saeki, E., Wada, A., & Fujimoto, M. (1988, August). Properties of brace encased in buckling-restraining concrete and steel tube. In Proceedings of ninth world conference on earthquake engineering (Vol. 4, pp. 719-724).

Wu, S., He, H., Lan, B., & Chen, Y. (2023). Seismic optimization design of buckling-restrained braced frames for uniform damage criterion. Journal of Constructional Steel Research, 208, 107992.

Yang, C. S. W., DesRoches, R., & Leon, R. T. (2010). Design and analysis of braced frames with shape memory alloy and energy-absorbing hybrid devices. Engineering Structures, 32(2), 498-507.

Yun, S. Y., Hamburger, R. O., Cornell, C. A., & Foutch, D. A. (2002). Seismic performance evaluation for steel moment frames. Journal of Structural Engineering, 128(4), 534-545.